Journal of Catalysis 267 (2009) 129–139

Contents lists available at ScienceDirect

Journal of Catalysis

journal homepage: www.elsevier.com/locate/jcat

Development of the HYD route of hydrodesulfurization of dibenzothiophenes over Pd–Pt/γ-Al_2O_3 catalysts

V.G. Baldovino-Medrano [a], P. Eloy [b], E.M. Gaigneaux [b], Sonia A. Giraldo [a], Aristóbulo Centeno [a,*]

[a] Centro de Investigaciones en Catálisis (CICAT), Escuela de Ingeniería Química, Universidad Industrial de Santander (UIS), Cra. 27 Calle 9, Bucaramanga, Colombia
[b] Université catholique de Louvain, Unité de catalyse et chimie des matériaux divisés, Croix du Sud 2/17, B-1348 Louvain-la-Neuve, Belgium

ARTICLE INFO

Article history:
Received 1 April 2009
Revised 3 August 2009
Accepted 3 August 2009
Available online 17 September 2009

Keywords:
Pd–Pt/γ-Al_2O_3
Pd/(Pd+Pt) molar ratio
Dibenzothiophene hydrodesulfurization
HYD route mechanism
$Pd^{\delta+}$ surface species

ABSTRACT

The hydrodesulfurization (HDS) of dibenzothiophene (DBT) on a series of Pd–Pt/γ-Al_2O_3 catalysts was studied as a function of the Pd/(Pd + Pt) molar ratio at different reaction conditions. It was determined that the catalytic performance in HDS is controlled by the Pd/(Pd + Pt) molar ratio. In particular, a synergetic effect exists rather in the development of the hydrogenation (HYD) route of HDS of dibenzothiophene than in the activity, but both can be controlled from the Pd/(Pd + Pt) molar ratio. An analysis of the relationship between the mechanism of HYD, analyzed here from a different perspective as that currently presented in the literature, and the surface properties of the bimetallic Pd–Pt alloyed particles indicated that: (i) the development of HYD is in correspondence with the capacity of Pd–Pt to hydrogenate aromatics under HDS environments; (ii) the dispersion of the active phase is not directly related to the performance in HDS. Consequently, other geometric effects are more important to the development of HYD over Pd–Pt; and (iii) $Pd^{\delta+}$ surface species of the Pd–Pt alloyed particles are responsible for the hydrogenation–dehydrogenation steps during HYD, whereas C–S–C bond scission mainly takes place on Pt sites.

1. Introduction

The hydrodesulfurization (HDS) of dibenzothiophenes (DBTs) normally takes place by the parallel and competitive direct desulfurization (DDS) and hydrogenation (HYD) pathways [1–3]. The HDS of sterically hindered 4,6-alkyl-substituted-dibenzothiophenes (4,6-alkyl-DBTs), bull's eye in the HDS of heavy oil cuts, proceeds almost exclusively by the hydrogenation route [1–3]. Different authors have studied the HYD route [4–16]. HYD theoretically involves the formation of a π complex and multipoint interactions of the benzenic (η^6) and thiophenic (η^5) rings as well as the S heteroatom (η^1S) of the adsorbed molecule with the catalytic surface [4–8]. On the other hand, the hydrodesulfurization of 4,6-alkyl-DBTs via DDS is not an energetically favored process [4,12]. Regardless of the HDS pathway, DDS or HYD, it is believed that the C–S–C bond scission step can take place by the same mechanism [5,6,9,13]. According to the literature such mechanism can be direct hydrogenolysis of the C–S–C bond [6,9] or an elimination mechanism in which dihydrodibenzothiophenic intermediates are involved [6,13] or perhaps a combination of both [6,11]. An analysis of the published information indicates that DDS and HYD are kinetically competitive [1–16]. Such competition has been clearly evidenced when performing the HDS of dibenzothiophenes over supported MoS_2 and Pd [9,13–16]. In the case of promoted MoS_2 catalysts, it has been demonstrated that the addition of promoters enhances the HDS activity mostly by favoring DDS [16,17]. Even highly hydrogenating metals such as Pt present such promoting effect on MoS_2 [17]. This is the main reason of the poor efficiency of these catalytic systems in the HDS of 4,6-alkyl-DBTs. Reinhoudt et al. [18] compared the activity in the HDS of 4,6-alkyl-DBTs of γ-Al_2O_3 and amorphous alumino silicate (ASA) supported promoted MoS_2 and Pd–Pt catalysts. The rate of HDS of such molecules over Pd–Pt/ASA catalysts was fivefold higher than that of MoS_2-based systems [18]. The results presented in various reports show that this is related to the capacity of the alloyed Pd–Pt bimetallic system to develop the HYD route of HDS of the sterically hindered dibenzothiophenes [9,19]. The reasons for such capacity are not fully established yet, though some characteristics of the Pd–Pt active phase in hydrotreatment reactions have been started to be elucidated [19,20].

Aiming the rational design of an efficient catalytic system for the HDS of sterically hindered 4,6-alkyl-DBTs, in the present contribution a series of Pd–Pt/γ-Al_2O_3 catalysts of different Pd/(Pd + Pt) atomic ratios were prepared and tested in the HDS of dibenzothiophene under different reaction conditions. By choosing DBT as a model molecule, instead of the more typically selected 4,6-dimethyl-DBT, it can be really established whether the studied

* Corresponding author. Fax: +57 7 6344684.
E-mail address: acenteno@uis.edu.co (A. Centeno).

0021-9517/$ - see front matter © 2009 Elsevier Inc. All rights reserved.
doi:10.1016/j.jcat.2009.08.004

catalytic system is intrinsically selective to HYD or DDS, because, as discussed above, the HDS of dibenzothiophene is not driven by the steric effect imposed by the methyl substituents in the 4- and 6-β-carbons, thus being possible to analyze the kinetic competition between both reaction pathways. To accomplish the proposed objective, we have performed an analysis of the mechanism of HYD of dibenzothiophenes over Pd–Pt based on the obtained results and the findings reported in the literature correlating it with the physicochemical characteristics of the alloyed Pd–Pt particles as determined by H_2 and CO chemisorption measurements, XPS, and TPR characterization. This work then contributes to the understanding of the HYD mechanism and casts new light into the nature and functioning of the Pd–Pt active phase in HDS.

2. Experimental

2.1. Catalysts preparation

A series of bimetallic Pd–Pt/γ-Al_2O_3 catalysts of different Pd/(Pd + Pt) molar ratios were prepared by incipient wetness co-impregnation. The alumina (*Procatalyse*) was crushed and sieved up to a particle size between 0.3 and 0.6 mm and then it was calcined at 673 K. An aqueous solution of $PdCl_2$ and $H_2PtCl_6{\cdot}4H_2O$ (both provided by Sigma-Aldrich), containing the desired amounts of Pt and Pd, was prepared and impregnated onto the support using a 20% excess of the impregnating solution as referred to the support's pore volume. The wetted solid was dried at ambient conditions for one day. Then, it was dried at 393 K for 12 h and calcined at 773 K for 4 h in air flow. The Pd/(Pd + Pt) molar ratio was varied from 0 (pure Pt) to 1 (pure Pd). Catalysts were labeled according to their real metallic contents as shown in parenthesis after the corresponding metal.

2.2. Catalysts characterization

2.2.1. Metallic contents and textural properties

The metallic contents of the catalysts were established by atomic absorption technique in a 2380 Perking Elmer spectrometer following the ASTM 1977-91 standard. These metallic contents are included in catalyst's labels as described in Section 2.1. BET surface area, pore volume, distribution, and pore size, using the BJH method, were determined by nitrogen adsorption–desorption isotherms in a Nova 1300 (Quantachrome) apparatus.

2.2.2. Hydrogen chemisorption

Hydrogen chemisorption measurements were performed in a Micromeritics ASAP 2010C instrument. All catalysts were in situ reduced in hydrogen at 673 K before the measurements. After this step, evacuation was performed by flowing He for 2 h at 673 K, under vacuum at 673 K for 30 min, and finally under vacuum at the temperature selected for the measurement for another 30 min. Hydrogen chemisorption isotherms were determined at 343 K to avoid the formation of the β-Pd–H hydride phase [21], this was also verified by TPR measurements. The reported hydrogen uptake values were taken from the volume difference between two hydrogen adsorption isotherms; the second one measured after an evacuation time of 45 min, extrapolated to zero pressure (strongly adsorbed hydrogen). For the calculation of dispersion from these measurements the ratio H/M = 1 was assumed between the metallic phases (Pd, Pt and Pd–Pt) and hydrogen.

2.2.3. CO chemisorption

CO chemisorption measurements were conducted on a Micromeritics Pulse Chemisorb 2700 apparatus. Samples of the calcined catalysts, c.a. 0.15 g, were dried using hydrogen (30 mL/min) at 393 K and subsequently at 493 K during 30 min at each temperature before performing its final reduction under the same hydrogen flow at 673 K for 2 h. At this same temperature, helium (30 mL/min) was flowed into the system during 90 min. The system was then cooled down to 318 K at which CO pulses were repeatedly injected until saturation of the sample. Dispersion was determined according to the procedure presented by Hermans et al. [22]. For the monometallic catalysts the ratios CO/Pt = 1 and CO/Pd = 0.68 were assigned as recommended by Navarro et al. [23]. For the bimetallic Pd–Pt catalysts the stoichiometric factor was calculated according to the formula: $X_{Pt}{*}1 + X_{Pd}{*}0.68$, where X is the molar fraction of the metal in the alloy.

2.2.4. Temperature-programmed reduction (TPR)

Temperature-programmed reduction (TPR) experiments were performed in a u-shaped fixed-bed quartz micro-reactor containing samples of c.a. 100 mg of the calcined catalysts to which a layer of approximately 1 cm of glass beads was added to guaranty plug-flow. Before the analysis, drying of the samples under He flow (50 mL/min) was performed at 413 K until stabilization of the H_2O signal as registered with a QMC 311 Balzers quadrupole mass spectrometer coupled to the reactor. After cooling the reactor, TPR patterns were then registered by increasing the temperature from 308 K to 1073 K at a temperature rate of 10 K/min. TPR analysis was performed by flowing a 5 vol.% H_2 in He (flow rate = 50 ml/min) gas mixture. The MS signals corresponding to H_2 ($m/e = 2$), H_2O (m/e;= 18), HCl ($m/e = 36$), and Cl^+ ($m/e = 37$); corresponding to diverse chlorine containing compounds, were monitored. The recorded signals were treated by using a Gaussian mathematical function.

2.2.5. X-ray photoelectron spectroscopy (XPS)

XPS analyses were performed with a Kratos Axis Ultra spectrometer (Kratos Analytical – Manchester – UK) equipped with a monochromatized aluminum X-ray source (powered at 10 mA and 15 kV). The sample powders were pressed into small stainless steel troughs mounted on a multi-specimen holder. The pressure in the analysis chamber was around 10^{-6} Pa. The angle between the normal to the sample surface and the lens axis was 0°. The hybrid lens magnification mode was used with the slot aperture resulting in an analyzed area of 700 μm × 300 μm. The pass energy was set at 40 eV. In these conditions, the energy resolution gives a full width at half maximum (FWHM) of the Ag 3 $d_{5/2}$ peak of about 1.0 eV. Charge stabilization was achieved by using the Kratos Axis device. The following sequence of spectra was recorded: survey spectrum, C 1s, O 1s, Al 2p, Al 2s, Pd 3d, Pt 4d, Cl 2p, and C 1s again to check the stability of charge compensation in function of time and the absence of degradation of the sample during the analyses. The binding energies were calculated with respect to the C-(C,H) component of the C 1s peak fixed at 284.8 eV. The spectra were decomposed with the CasaXPS program (Casa Software Ltd., UK) with a Gaussian/Lorentzian (70/30) product function after subtraction of a linear baseline. Molar fractions were calculated using peak areas normalized on the basis of acquisition parameters, sensitivity factors provided by the manufacturer, and the transmission function. The Pd 3d doublet was decomposed in three components with Pd $3d_{5/2}$ binding energies fixed at 335 (Pd^0), 336 (Pd^{2+}), and 338 eV (Pd^{4+}) [24]. The algebraic sum of the surface atomic concentration of ($Pd^{2+} + Pd^{4+}$) species was defined as the total concentration of surface electron-deficient $Pd^{\delta+}$ species. For the Pt 4d peak the energy separation for the doublet was fixed at 16.8 eV [25].

2.3. Catalytic tests

Catalytic tests were carried out in a continuous-flow high-pressure fixed-bed reactor. Catalysts were in situ activated before catalytic tests. Samples of 0.5 g of the calcined catalysts were dried at 393 K under N_2 flow for 1 h, and subsequently, they were reduced in hydrogen flow (100 mL/min) at 673 K for 3 h. The HDS of DBT (2 wt.%) was studied at 583 K, 5 MPa, and using a H_2/(liquid feed) ratio of 500 NL/L. DBT was diluted in cyclohexane. For all the tests, catalysts were diluted in borosilicate glass beads (1 mm in diameter, Aldrich) and placed between two glass wool plugs. The absence of any diffusion limitations was previously verified. Liquid products were analyzed using a HP 6890 GC equipped with an FID, a HP-1 capillary column (100 m × 0.25 mm × 0.5 μm), and a split injector. Catalytic tests were conducted until reaching the steady state. Hexadecane was employed as an internal standard for GC analysis of reaction products. In addition, the influence of reaction temperature, within the range 563–603 K, was studied for the monometallic Pt and Pd catalysts.

The catalyst with a Pd/(Pd + Pt) molar ratio of 0.8, Pd(1.0)–Pt(0.5), was selected for a long-run test. This test consisted on performing the HDS of dibenzothiophene until reaching steady state and then adding NP (3 wt.%) to the liquid feed. Once a new steady state was reached, dimethyldisulfide (DMDS) was incorporated to the feed as to generate an additional H_2S concentration of c.a. 4074 wppm, such H_2S concentration corresponding to the one obtained at 60% conversion of DBT in the hydrodesulfurization reaction. When stable conversions were achieved, DMDS was withdrawn from the system, closing the cycle which began with NP addition. As described, this experiment allows studying the influence of the incorporation of NP to a stabilized Pd–Pt catalyst on the performance in the HDS of dibenzothiophene, as well as the influence of an increase in the H_2S concentration on the simultaneous HDS–naphthalene hydrogenation reaction thus performed.

The catalytic results were expressed in terms of the conversion (%C) of DBT or NP:

$$\%C_i = 100 \times \frac{(n_0^i - n_f^i)}{n_0^i}; \quad (1)$$

where n_0^i and n_f^i are the initial and final moles irrespective of DBT or NP, and as the yield (%y) of products:

$$\%y_j = 100 \times \frac{n_j}{n_{\mathrm{DBT},0}}, \quad (2)$$

where n_j are the moles of different reaction products: cyclohexylbenzene (CHB), biphenyl (BP), tetrahydro(TH)–DBT (THDBT), and hexahydro(HH)–DBT (HHDBT), and $n_{\mathrm{DBT},0}$ are the initial moles of DBT, respectively. Such definition was adopted from IUPAC recommendations [26].

The selectivity ($S_{\mathrm{HYD}}^{\mathrm{DS}}$) between completely desulfurized CHB and BP in the HDS of dibenzothiophene was defined as the $y_{\mathrm{CHB}}/y_{\mathrm{BP}}$ ratio, i.e. the ratio moles of CHB to moles of BP. The experimental error in the mass balance of the reaction system, as from the chromatography analysis, and the reproducibility of the catalytic tests was found to be between 10% and 15%.

Activation energy calculations (E_a) for the conversion of DBT over monometallic Pt and Pd were performed by assuming a pseudo-first order rate constant, as in previous works [15,17], and by linearization of the Arrhenius expression.

3. Results and discussion

The catalytic trends and the characteristics of the Pd–Pt active phase in the HDS of dibenzothiophene as a function of the Pd/(Pd + Pt) molar ratio are analyzed first. Afterwards, the analysis is focused on the trends observed during the long-run test.

3.1. HDS of dibenzothiophene

Reaction products detected in these tests were: CHB, BP, and partially hydrogenated THDBT and HHDBT.

3.1.1. Effect of temperature on the HDS of dibenzothiophene over monometallic Pt and Pd

Table 1 shows the effect of the reaction temperature on the activity ($\%C_{\mathrm{DBT}}$) and the reaction products distribution for monometallic Pd(1.9) and Pt(1.3), and the activation energy values determined. For both catalysts $\%C_{\mathrm{DBT}}$ increased with temperature. The activation energies were in the same order of magnitude of those usually reported in the literature when no diffusion limitations are present [27]. As observed in Table 1, Pt was much more active than Pd, which agrees with the literature reports [14,18,19]. Regarding products distribution, it can be seen that this was quite different for Pt compared to Pd. While for Pt most of the DBT was converted to biphenyl, i.e. very high selectivity to DDS, for Pd the sum of the yields of the products from the HYD route, CHB, THDBT, or HHDBT, was always at the same level than that of BP. In particular, the yields of both desulfurized products, i.e. CHB and BP, increased with temperature over both catalysts, with BP as the main reaction product. For Pt the yield of BP was an order of magnitude higher than that of CHB indicating a very high selectivity to DDS. This trend has also been found by other authors [14,28,29]. Over Pd, the yield to CHB was c.a. half the corresponding BP value. Both partially hydrogenated intermediates, THDBT and HHDBT, were observed for Pd, and instead over Pt only a very low amount of THDBT was detected. It must be recalled that for the HDS of dibenzothiophene, thermodynamic calculations presented in literature [19,27] indicate that at the temperature range and pressure used in this work, the production of BP is favored, and that the increase in the temperature negatively affects the reactions of saturation of aromatic rings to a higher extent than the C–S–C bond scission reaction [19]. A noticeable difference between Pt and Pd is that over the former the yield of THDBT decreased with rising temperature while over Pd it increased. The trend observed for THDBT over Pt was similar to that registered for HHDBT over Pd; though in this case such decrease was very slight. The above-mentioned trends clearly indicate that while over Pt the HDS reaction proceeds with a selectivity as predicted from thermodynamics, over Pd there is a significant kinetic competition between the HYD and DDS pathways. Therefore, the chemical properties of the noble metals are playing a role in controlling the selectivity in HDS.

3.1.2. The HYD mechanism of hydrodesulfurization of dibenzothiophenes

The results for the HDS of dibenzothiophene over both monometallic Pt and Pd catalysts showed that, under the conditions used in this work, HYD is kinetically slower than DDS and becomes more competitive to the latter on those catalysts displaying lower HDS rates; as for unpromoted MoS_2 [10,11,16].

Up to date, the mechanism of DDS remains an object of controversy, because evidence supporting an elimination type mechanism and/or direct C–S–C bond hydrogenolysis has been extensively documented [5,6,9–13,16]. However, there is a good agreement in the fact that the same mechanism can operate either in DDS or in the final C–S–C bond scission step of HYD [6,7,9,12,13,16]. For HYD, it has been proposed that a π-complex between the catalyst active phase and the DBT backbone is formed leading to the sequential saturation of one of the benzenic rings of DBT [4–8]. Literature reports indicate that such π-complex is

Table 1
Effect of reaction temperature on the HDS of dibenzothiophene over monometallic γ-Al_2O_3-supported Pd and Pt catalysts.

Catalyst[a]	Temperature (K)	$\%C_{DBT}$	$\%y_{THDBT}$	$\%y_{HHDBT}$	$\%y_{CHB}$	$\%y_{BP}$	E_a (kJ/mol)[b]
Pt(1.3)	563	50.4	1.9	0	3.6	45.9	77.2
	583	69.2	1.0	0	5.3	63.2	
	603	87.7	0.5	0	7.1	80.1	
Pd(1.9)	563	17.9	4.8	1.5	3.7	7.8	58.6
	583	25.9	5.7	1.4	6.2	12.5	
	603	36.4	6.6	1.2	10.2	18.3	

[a] Numbers in parentheses indicate metallic contents (wt.%).
[b] Activation energy calculated from Arrhenius expression assuming pseudo-first order rate constant.

formed by flat adsorption (also called π adsorption) of the DBT molecule on the catalytic surface, and that, in this way, the interaction between both is not only restricted to that of the π bonds of the benzenic rings (η^6 mode) but also includes the π bonds of the thiophenic ring (η^5 mode) and even the (η^1S) mode of coordination of the surface with the S heteroatom of the adsorbed molecule [4–8]. Though these results have been presented for MoS_2 catalysts, it can be expected that the same kind of interactions can occur between dibenzothiophene and the active phase of the Pd–Pt catalysts. Considering this evidence a mechanism for the HYD route of hydrodesulfurization of dibenzothiophenes can be regarded as a dynamic competition between hydrogenation–dehydrogenation reactions of the benzenic ring of DBT, i.e. between DBT, THDBT, and HHDBT, and the scission of the C–S–C bond of the thiophenic ring. Where, the use of the term dynamic implies that DBT and the different reaction intermediates are interacting with the active surface in such a way that the former can be adsorbed and desorbed several times during the reaction. The experimental evidence presented by Prins and co-workers [9–11,14,30] aiming to establish the mechanism of C–S–C bond scission in HDS points out in the same direction of the present proposition, where these authors suggested that the hydrogenolysis of the C–S–C bond of the reaction intermediates in the HDS dibenzothiophenes proceeds after their re-adsorption in a perpendicular σ-mode through the S heteroatom. The present proposition is also compatible with the elimination mechanism of C–S–C bond scission proposed by other authors as well [6,13,31]. Within this frame, it must be said that as the resonance energy of the aromatic rings decreases from DBT to THDBT and then to HHDBT the C–S–C bond scission reaction becomes subsequently more kinetically favored than the hydrogenation–dehydrogenation reactions. Indeed, recent results by Wang and Prins [11] have demonstrated that the S heteroatom is more rapidly withdrawn from HHDBT than from THDBT and DBT. However, the rate of interconversion between THDBT and HHDBT can be significant for Pd [11], but such hydrogenation–dehydrogenation reaction is known to result in an equilibrium between both partially hydrogenated intermediates [11,32]. The hydrogenation of THDBT to HHDBT can lead to either *trans*-HHDBT or *cis*-HHDBT [13,33], therefore it is also possible that the *cis*- to *trans*-stereoselectivity could be playing a role in the suggested HYD mechanism when considering a C–S–C bond scission step proceeding via elimination.

3.1.3. Relationship between the HYD route of hydrodesulfurization and aromatics hydrogenation

Metallic Pd catalysts are highly selective to *trans*-isomers in aromatics hydrogenation [15,34–36]. This implies a strong interaction between its hydrogenation active sites and the aromatic rings, because to produce *trans*-isomers the aromatic molecule must theoretically turn over the catalytic surface as to comply the condition of addition of atomic H by the same side of the molecule [34]. Therefore, from the theoretical point of view, when *trans*-isomers are produced during a reaction, the adsorbed intermediates necessarily change their mode of coordination to the catalytic surface. Dokjampa et al. [35] related such mechanism to a slower rate of transfer of activated atomic H from the active phase of supported metallic catalysts to the π-unsaturated double bonds of the aromatics [35]. Indeed, Table 2 displaying the results of H_2 chemisorption for the prepared Pd–Pt catalysts shows that at the same temperature (343 K) the Pd(1.9) catalyst had a lower capacity to chemisorb H_2 than Pt(1.3). This is further evidenced because when lowering the temperature of the measurement for Pt(1.3), i.e. for $T = 308$ K, the amount of H_2 chemisorbed by this catalyst was then closer to the value exhibited by Pd(1.9) at $T = 343$ K. In general, the capacity to chemisorb H_2 by a supported metallic catalyst can be related to its capacity to activate H_2 and to transfer this activated hydrogen from the catalytic surface to the reactants [37]. The results of H_2 chemisorption for Pt(1.3) at 308 and 343 K indicate that the increase in temperature augments the capacity of Pt/γ-Al_2O_3 to chemisorb H_2 (Table 2). Moreover, as evidenced by the value of Pt dispersion as calculated from H_2 uptake at 343 K, which was higher than 100% (Table 2), it can be said that hydrogen spillover effects, which have been demonstrated to influence the catalytic properties of Pt/γ-Al_2O_3 [38,39], are playing a significant role in the performance of Pt/γ-Al_2O_3 in HDS. Though, it can be expected that the supported catalyst possess a maximum capacity to chemisorb H_2, when rising the temperature even if such maximum has been attained the rate of activation of H_2 and thus its rate of transfer to a reactant increases [37]. Therefore, under the conditions of the HDS catalytic tests, $T = 583$ K and $P = 5$ MPa, it can be assumed that a catalyst possessing a higher H_2 chemisorption capacity would be able to activate a higher amount of H_2, thus transferring it faster to reactants, having consequently a higher activity in hydrotreatment reactions as well as it can modify the stereoselectivity in aromatics hydrogenation. In this line of thought, considering the conversion of THDBT to *cis*-HHDBT or *trans*-HHDBT and making a comparison with the hydrogenation of non-sulfur-containing aromatic molecules, the differences in the H_2 chemisorption capacity of both supported Pt and Pd catalysts can be correlated with the mechanism of the HYD route of hydrodesulfurization of dibenzothiophenes. In first place, as observed in Table 1, Pt was highly active in the HDS of dibenzothiophene and very selective to DDS; this result being in agreement with previous reports [14,28,29]. In the absence of sulfur-containing molecules Pt is also very active in aromatics hydrogenation with very good selectivity to *cis*-isomers [34,35,40]. Concerning Pd/γ-Al_2O_3, in a previous work [15], we were able to correlate the stereoselectivity in aromatics hydrogenation with the HYD mechanism of HDS of dibenzothiophene. The high selectivity to *trans*-isomers of Pd was associated to a stronger interaction of the aromatics with the Pd active phase and to a lower rate of atomic H transfer from the metal to these rings; therefore, the particularly good selectivity of Pd to HYD, but its lower activity in HDS, was assumed to be a consequence of these two phenomena. The arguments discussed so far and the results obtained here support the hypothesis of an HYD mechanism proceeding in a similar

Table 2
H_2 and CO chemisorption results for the prepared Pd–Pt/γ-Al_2O_3 catalysts.

Catalyst[a]	Chemisorption				
	n_{ads}^{STP} (μmol/μmol metal)		No. of μ moles of accessible metal per reaction[b]	%Dispersion	
	H_2 (343 K)	CO (308 K)		H_2	CO
Pt(1.3)	0.19[c]	0.37	4.5	38[c]	37
	0.57			114	
Pd(0.2)–Pt(1.5)	0.22	0.45	9.6	44	37
Pd(0.9)–Pt(0.7)	0.26	0.37	7.4	51	30
Pd(1.0)–Pt(0.5)	0.29	0.37	7.8	57	30
Pd(1.4)–Pt(0.3)	0.17	0.25	4.6	33	21
Pd(1.9)	0.10	0.20	3.5	21	14

[a] Numbers in parentheses indicate metallic contents (wt.%) as determined by atomic absorption.
[b] Determined from CO chemisorption measurements.
[c] Measured at 308 K.

way to aromatics hydrogenation in the sense of the occurrence of a *roll-over* of DBT and its partially hydrogenated intermediates over the catalytic surface [15].

3.1.4. The reactivity of dibenzothiophene over bimetallic Pd–Pt catalysts

Table 3 shows the Pd/(Pd + Pt) molar ratios and textural properties of the prepared Pd–Pt catalysts. It can be seen that the textural properties of the catalysts were not very different from those of the bare γ-Al_2O_3 support. These results show that the incorporation of Pd and Pt to the support did not negatively influence the final textural properties of the catalysts, in spite of the strong pH (pH 0–1) of the impregnating solutions prepared from chlorides which can cause alumina dissolution during catalysts' preparation [41]. Consequently, an effect of the textural properties on the catalytic performance can be discarded. The reactivity of dibenzothiophene was controlled by the Pd/(Pd + Pt) molar ratio.

Fig. 1 displays both $\%C_{DBT}$ and S_{HYD}^{DS} as a function of the Pd/(Pd + Pt) molar ratio at 583 K. Concerning the catalytic activity, the trend registered in Fig. 1 led to conclude that the Pd–Pt alloys have low or no synergy effects regarding the HDS activity. In fact, it can be observed that those catalysts with higher Pt contents, Pd/(Pd + Pt) molar ratio = 0.2 and 0.6, were more active than the one containing the highest Pd load, Pd/(Pd + Pt) = 0.9. At a Pd/(Pd + Pt) molar ratio of 0.8 the highest activity among the bimetallic catalysts was registered, but without surpassing that of monometallic Pt. The selectivity to the HYD route of hydrodesulfurization also changed as a function of this variable, S_{HYD}^{DS}, increased with the Pd content (Fig. 1) until a maximum, $S_{HYD}^{DS} \approx 1$, located at the same Pd/(Pd + Pt) molar ratio as the maximum in activity. Analyzing the trend in S_{HYD}^{DS} a strong synergetic effect regarding the development of the HYD route was found. In this sense, the catalytic behavior of Pd–Pt in the development of the HYD route of reaction resembles that in aromatics hydrogenation under H_2S atmospheres [19,42,43]. Comparing the hydrogen uptake of the Pd–Pt alloys with that corresponding to the monometallic Pt and Pd catalysts (Table 2), at the same temperature (343 K), it is observed that

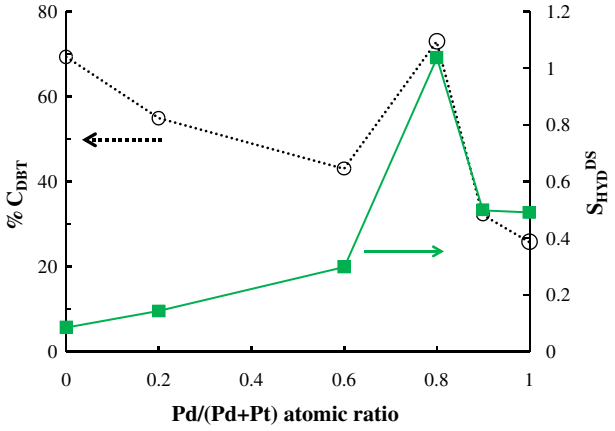

Fig. 1. Steady state activity ($\%C_{DBT}$) and selectivity cyclohexylbenzene to biphenyl (S_{HYD}^{DS}) for Pd–Pt/γ-Al_2O_3 catalysts in the hydrodesulfurization of DBT as a function of the Pd/(Pd + Pt) molar ratio. (○) $\%C_{DBT}$; (■) S_{HYD}^{DS}. Reaction conditions: T = 583 K, P = 5 MPa, liquid feed flow 30 mL/h, H_2/liquid feed ratio = 500 NL/L.

the alloyed catalysts had a higher H_2 chemisorption capacity than monometallic Pd, with a maximum located at Pd/(Pd + Pt) molar ratio = 0.8, but compared to Pt all the alloys chemisorbed lower amounts of hydrogen. If one compares the catalytic results (Fig. 1) with the H_2 uptake of the bimetallic catalyst (Table 2), it can be observed that in spite of the lower Pt content of monometallic Pt(1.3) compared to Pd(0.2)–Pt(1.5), the latter was less active with a slightly higher S_{HYD}^{DS} and chemisorbed a much lower amount of H_2 at the same temperature. On the other hand, starting from the monometallic Pd(1.9), low amounts of Pt in the bimetallic Pd–Pt catalysts increased H_2 uptake: Pd(1.0)–Pt(0.5) > Pd(0.9)–Pt(0.7) > Pd(1.4)–Pt(0.3) > Pd(1.9). A particularity in this trend is that until a Pt metallic content of 0.5 wt.%, i.e. Pd(1.0)–Pt(0.5), the increase in H_2 uptake was in good correspondence with the increase in S_{HYD}^{DS}. Though for monometallic Pt and Pd a relationship between H_2 uptake and the mechanism of HDS of dibenzothio-

Table 3
Textural properties of the prepared Pd–Pt/γ-Al_2O_3 catalysts as measured by nitrogen adsorption isotherms.

Catalyst	Pd/(Pd + Pt) molar ratio	BET surface area (m^2/g)	Average pore diameter (Å)	Pore volume (cm^3/g)
γ-Al_2O_3	–	211.4	111.9	0.6
Pt(1.3)	0.0	196.9	111.1	0.6
Pd(0.2)–Pt(1.5)	0.2	196.4	112.0	0.5
Pd(0.7)–Pt(0.9)	0.6	199.9	111.0	0.6
Pd(1.0)–Pt(0.5)	0.8	199.2	112.0	0.6
Pd(1.4)–Pt(0.3)	0.9	205.6	111.1	0.6
Pd(1.9)	1.0	200.6	109.8	0.6

phene was inferred; for the bimetallic Pd–Pt system the results indicated that such relationship is not very straight. Thus other factors must be considered, which will be discussed later. Fig. 2 shows the distribution of the reaction products (at 583 K) as a function of the Pd/(Pd + Pt) molar ratio. Special attention must be paid to the fact that for monometallic Pd the algebraic sum of the yields of CHB, THDBT, and HHDBT was slightly higher than the one corresponding to BP. Moreover, Pd yielded similar amounts of partially hydrogenated products and CHB (Fig. 2 and Table 1). From the standpoint of the addition of Pt to the system, this effect can be regarded as the presence of a small amount of this metal on the Pd-rich alloyed particles simultaneously accelerating both the hydrogenation of the DBT aromatic backbone and the extraction of the S heteroatom from DBT, THDBT, and/or the HHDBT intermediates so as to produce CHB. Further hydrogenation of BP to CHB can be neglected [44]. In conclusion, it can be thus said that the Pd/(Pd + Pt) molar ratio of the bimetallic catalysts can modify the competition between the hydrogenation–dehydrogenation-C–S–C bond scission reactions occurring during the HDS of dibenzothiophene.

3.2. Characteristics of the Pd–Pt active phase in dibenzothiophene HDS

A first issue to be discussed is the influence of dispersion on the reactivity of DBT over Pd–Pt. Subsequently, the surface chemical properties of Pd–Pt and its relationship with the reactivity of DBT over them will be discussed.

3.2.1. Relationship between dispersion and the reactivity of DBT over Pd–Pt catalysts

As discussed in Section 3.1.3, in this work it was opted for not using the dispersion obtained from H_2 chemisorption measurements due to the overestimation of its values from this technique. Therefore, dispersion was only considered from the results obtained by CO chemisorption measurements (Table 2). The adopted stoichiometry for Pd [23] and the Pd–Pt alloys is in agreement with the fact that CO can be adsorbed in both linear and bridge mode over Pd particles [45] and considering the composition of the alloys. Not all of the catalysts had the same dispersion. Dispersion decreased in the order: Pt(1.3) = Pd(0.2)–Pt(1.5) > Pd(0.9)–Pt(0.7) = Pd(1.0)–Pt(0.5) > Pd(1.4)–Pt(0.3) > Pd(1.9). The trend observed shows that, with the exception of the Pd(1.0)–Pt(0.5) catalyst, the increase in the concentration of Pd in the bimetallic Pd–Pt catalysts led to a decrease in the dispersion of the Pd–Pt particles over the γ-Al_2O_3 support. By comparing dispersion (Table 2) with the catalytic results in HDS (Figs. 1 and 2) no apparent correlation exists between them. The same has been reported by Niquille-Röthlisberger and Prins [14] for the HDS of dibenzothiophenes over Pd–Pt/γ-Al_2O_3. Focusing the present analysis on the development of the HYD route it must be remarked that though the hydrogenation–dehydrogenation reactions implicated in the HYD mechanism are considered to be structure-insensitive [46], this is not the case of the reactions leading to the scission of the C–S–C bond [47]. Consequently, the present results indicate that other geometrical effects are playing the central role in controlling the catalytic performance of the Pd–Pt system in the HDS of dibenzothiophenes. Indeed, geometric effects have been found to control to a great extent the catalytic properties of bimetallic Pd–Pt catalysts [48–50]. In the case of HDS, the theoretical work made by Jiang et al. [50] highlighted the influence of the structural conformation and composition of Pd–Pt alloyed particles in the interactions established between them and H_2 and H_2S. Depending on the arrangement of the Pd and Pt atoms in the bimetallic Pd–Pt clusters the adsorption, dissociation, and migration of hydrogen species, H_2S, and the S atom change [50]. Within a specific atomic ratio range the adsorption of H_2 became more favorable than the adsorption of H_2S over the bimetallic surfaces [50]. These theoretical results help explaining the high dependence of the activity in the HDS of dibenzothiophene and the synergy in the development of the HYD route on the Pd/(Pd + Pt) molar ratio discussed before.

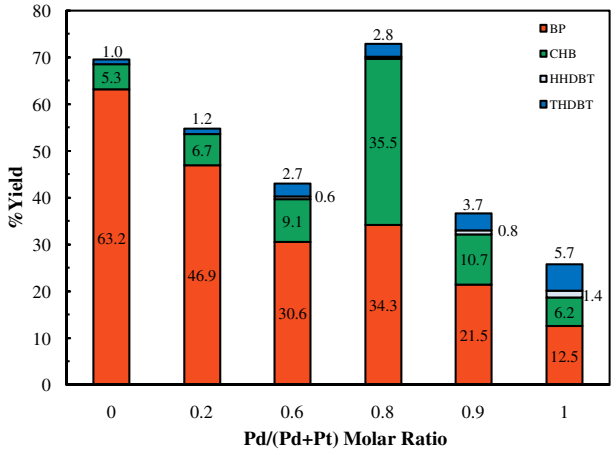

Fig. 2. Steady state products distribution for Pd–Pt/γ-Al_2O_3 catalysts in the desulfurization of DBT as a function of Pd/(Pd + Pt) molar ratio. THDBT: tetrahydrodibenzothiophene; HHDBT: hexahydrodibenzothiophene; BP: biphenyl; CHB: cyclohexylbenzene.

3.2.2. Surface chemical properties of Pd–Pt catalysts and the development of the HYD route of HDS of dibenzothiophenes

The results of the XPS characterization of both the calcined and reduced, i.e. activated, catalysts are displayed in Table 4. The objective of characterizing the catalysts in these two states was to analyze the evolution of the chemical state and surface properties of the Pd–Pt particles. In this sense, a comparison of the XPS results of the Pd–Pt catalysts in these two states showed that after reduction there was a decrease in the surface Pd/(Pd + Pt) atomic ratio of the bimetallic catalysts: precisely from 0.17, calcined, to 0.08, reduced, for Pd(0.2)–Pt(1.5), 0.55–0.31 for Pd(0.9)–Pt(0.7), 0.86–0.62 for Pd(1.0)–Pt(0.5), and 0.88–0.61 for Pd(1.4)–Pt(0.3), respectively. Thermodynamics calculations reported in the literature [19] indicate that at the conditions of temperature used during the calcination stage (T = 773 K) an alloy between Pd and Pt is readily formed. Therefore, the XPS analysis demonstrates that after activation the surface composition of the alloy changes. The decrease in the surface Pd/(Pd + Pt) atomic ratio of the alloys can be regarded as a signal of a migration of Pd to the outer surface of the alloy. This has been interpreted by some authors as a segregation of Pd atoms to the surface of the Pd–Pt particles [51]. Normally, the XPS analysis of Pd–Pt alloys is focused on detecting a shift in the BE of the Pd and/or Pt doublets [23,49] due to intermetallic interactions. However, such shifts are not usually significant as to draw conclusions. The results obtained here in this sense were similar. Fig. 3 shows the XPS spectra of monometallic Pt(1.3) (a) and bimetallic Pt(1.5)-Pd(0.2) (b) both calcined and after reduction. The positions of the Pt 4d and Pd 3d doublets did not display a large BE shift neither by the formation of the alloy between Pd–Pt nor after reducing the catalysts. The Pt 4d line in Pt(1.3) and Pd(0.2)–Pt(1.5) remained around 315–315.5 eV in all cases; monometallic and bimetallic catalysts whether calcined or reduced, while the Pd 3d line remained in the range 335–338 eV. The same trend was found for the other Pd–Pt/γ-Al_2O_3 catalysts. Taking into account that this is the same result presented in most literature reports, we decided instead to decompose the Pd 3d doublet into three components (see Section 2.2.5) and to study the evolution of the distribution of such components from the calcination to the reduced state of the catalysts. The results (Table 4) demonstrate that during reduc-

Table 4
XPS analysis of the Pd $3d_{5/2}$ peak of prepared Pd–Pt/γ-Al_2O_3 catalysts after calcination and reduction.

Catalyst	%At.						Surface atomic ratios				
Pd(1.9)	Pd 3d (Pd^0)	Pd 3d (Pd^{2+})	Pd 3d (Pd^{4+})	Pt 4d	Cl 2p	Al 2p–2s[a]	Pd/(Pd + Pt)	Pd/Al	Pt/Al	$Pd^{\delta+}/Pd^0$	Cl/Al
Calcined	0.04	0.13	0.05	–	0.59	36.25	1.00	0.006	–	4.02	0.016
Reduced	0.08	0.09	0.06	–	0.57	28.49	1.00	0.008	–	1.92	0.020
Pt(1.3)											
Calcined	–	–	–	0.29	0.62	24.76	0.00	–	0.012	–	0.025
Reduced	–	–	–	0.25	0.61	21.00	0.00	–	0.012	–	0.029
Pd(0.2)–Pt(1.5)											
Calcined	N.D.	0.04	N.D.	0.19	0.56	23.93	0.17	0.002	0.008	N.D.	0.023
Reduced	0.02	0.01	0.02	0.15	0.63	21.79	0.08	0.001	0.007	N.D.	0.029
Pd(0.9)–Pt(0.7)											
Calcined	0.03	0.07	0.02	0.11	0.51	24.77	0.55	0.005	0.004	2.83	0.021
Reduced	0.01	0.05	0.04	0.18	0.60	19.70	0.31	0.005	0.009	11.00	0.030
Pd(1.0)–Pt(0.5)											
Calcined	0.06	0.11	0.03	0.08	0.51	24.47	0.86	0.008	0.003	2.24	0.020
Reduced	0.01	0.15	0.07	0.05	0.70	20.74	0.62	0.011	0.002	17.80	0.034
Pd(1.4)–Pt(0.3)											
Calcined	0.08	0.13	0.04	0.03	0.60	24.60	0.88	0.010	0.001	1.96	0.024
Reduced	0.01	0.11	0.04	0.08	0.61	21.09	0.61	0.008	0.004	11.21	0.029

[a] For the Pt containing catalysts the Al 2s line was selected.

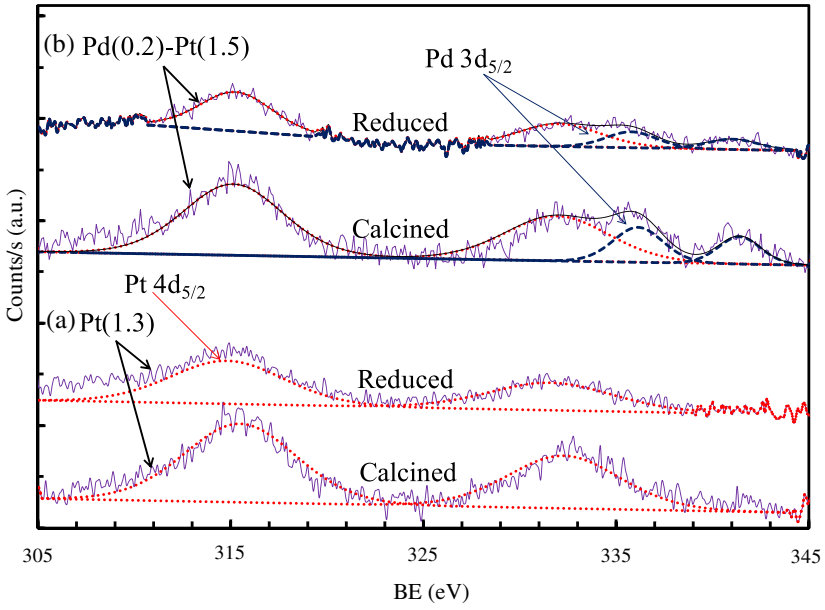

Fig. 3. XPS spectra of (a) Pt(1.3) and (b) Pd(0.2)–Pt(1.5); calcined and reduced samples, respectively. (···) Pt 4d; (---) Pd 3d.

tion there was a change in the proportions of metallic Pd^0 and electron-deficient Pd^{4+} and Pd^{2+} surface species. It can be seen that the $Pd^{\delta+}/Pd^0$ surface atomic ratio increased after reduction. The values of the $Pd^{\delta+}/Pd^0$ atomic ratio decreased in the order: Pd(1.0)–Pt(0.5) > Pd(1.4)–Pt(0.3) ≈ Pd(0.9)–Pt(0.7), where it was not possible to measure the $Pd^{\delta+}/Pd^0$ atomic ratio for the sample of Pd(0.2)–Pt(1.5) because of the low concentration of Pd. The catalyst Pd(1.0)–Pt(0.5) showed the highest increase in the amount of electron-deficient $Pd^{\delta+}$ species as compared to metallic Pd^0 ones after reduction. Of course, one may think that an increase in the $Pd^{\delta+}/Pd^0$ atomic ratio after reduction is an unexpected result. In fact, the surface $Pd^{\delta+}/Pd^0$ atomic ratio determined for the monometallic Pd catalyst decreased after reduction, which is due to reduction of the oxide Pd particles, but some $Pd^{\delta+}$ particles remain. The trends registered for the $Pd^{\delta+}/Pd^0$ atomic ratio can be associated to: (i) the intermetallic interaction between Pt and Pd in the bimetallic particles, and (ii) the influence of residual chlorine in the oxidation state of the metals.

In the case of an intermetallic interaction between Pt and Pd, the formation of an alloy between the metals is an important factor. The formation of a Pd–Pt alloy was confirmed by TPR results as shown in Fig. 4. That the TPR profile of the bimetallic samples, i.e. Pd(0.2)–Pt(1.5) Fig. 4c, Pd(0.9)–Pt(0.7) Fig. 4d, Pd(1.0)–Pt(0.5) Fig. 4e, and Pd(1.4)–Pt(0.3) Fig. 4f, was not the simple superposition of those corresponding to monometallic Pt(1.3) Fig. 4a and Pd(1.9) Fig. 4b. Pt displayed a wide reduction peak with a maximum located around 490 K and a small shoulder at 640 K as in agreement with other studies [52]. On the other hand, Pd exhibited a peak of hydrogen production around 336 K due to the decomposition of the β-Pd–H hydride phase [53]. The same peak was only detected again for the Pd(1.5)–Pt(0.2) bimetallic catalyst, but it was shifted to a lower temperature (320 K) Fig. 4f. This can be attributed to an inhibition of the formation of the β-Pd–H hydride phase due to Pt addition [54]. Comparing Pt and Pd it can be observed that the latter is more easily reduced than the former. As observed in Fig. 4c–f the H_2 consumption was lower for the bime-

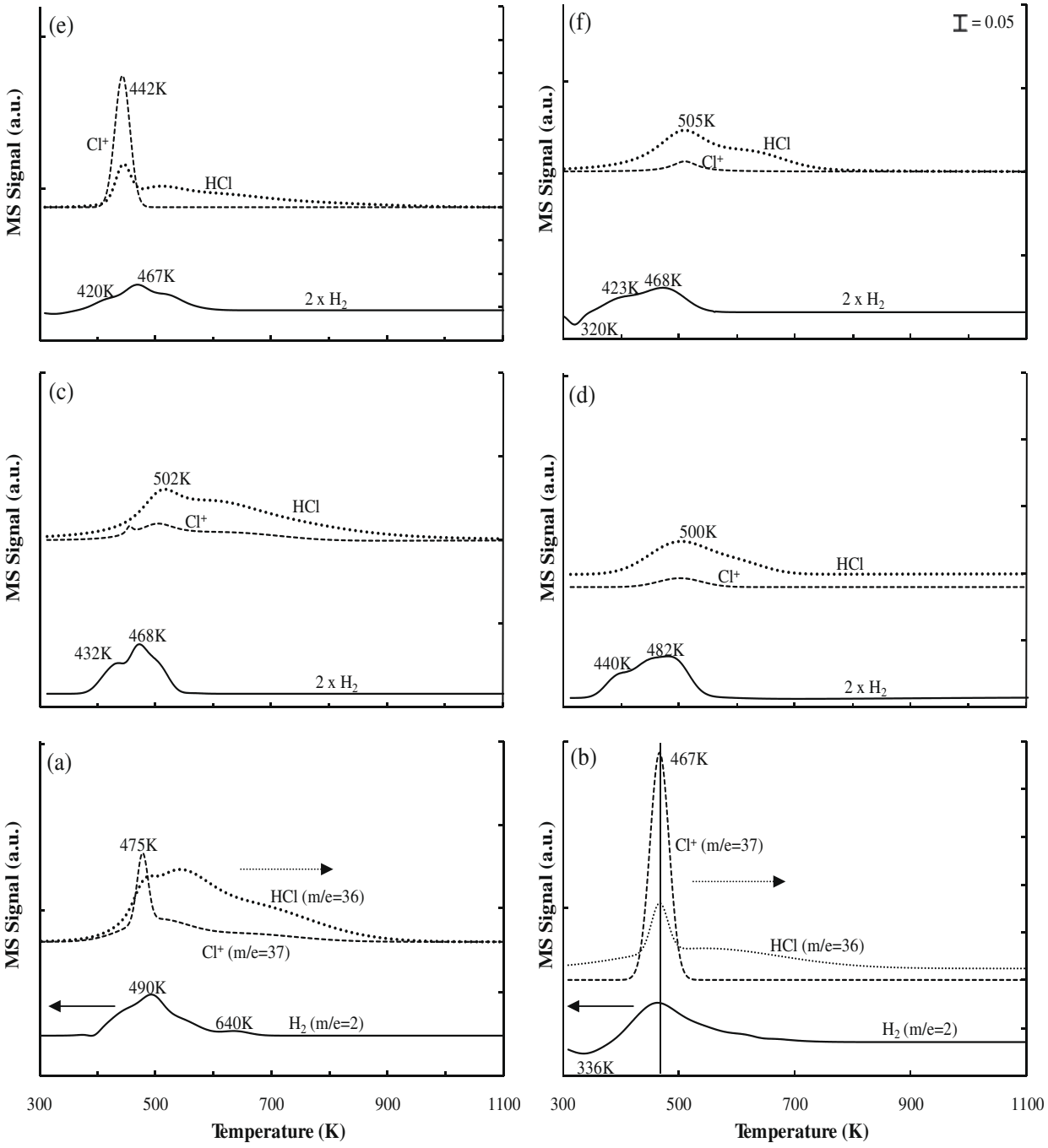

Fig. 4. Temperature-programmed reduction profiles for calcined catalysts: (a) Pt(1.3), (b) Pd(1.9), (c) Pd(0.2)–Pt(1.5), (d) Pd(0.7)–Pt(0.9), (e) Pd(1.0)–Pt(0.5), and (f) Pd(1.4)–Pt(0.3). H_2 consumption (primary axis), HCl and Cl^+ production (secondary axis) mass spectrometer signals vs. temperature.

tallic Pd–Pt/γ-Al_2O_3 catalysts than for monometallic Pt and Pd. With the exception of Pd(0.9)–Pt(0.7), the alloys exhibited a reduction maximum at the same temperature as monometallic Pd, i.e. around 467 K. It is not clear why the maximum in the H_2 signal of the Pd(0.9)–Pt(0.7) catalyst was located at a higher temperature but it evidences the complex nature of the interactions between both metals in the alloy. In conclusion, the TPR analysis performed demonstrates the formation of an alloy between Pd–Pt, where the reducibility of the Pd–Pt/γ-Al_2O_3 catalysts depends again on the Pd/(Pd + Pt) molar ratio. The changes in the surface $Pd^{\delta+}/Pd^0$ atomic ratio can, consequently, be the result of the formation of an ionic Pd–Pt bond of the metals within the alloy. After reduction, this Pd–Pt ionic bond can be strengthened leading to the increase in the concentration of $Pd^{\delta+}$ species observed in XPS. Some articles in the literature have actually discussed this phenomenon. For example, Bando et al. [55] studied the chemical state of Pd–Pt/γ-Al_2O_3 catalysts prepared from chlorides after calcination and after reduction by EXAFS. They found that the bands assigned to Pd-(O,Cl) and Pt-(O,Cl) tend to disappear after reduction and new bands assigned to metal–metal bonds: Pd–Pd, Pt–Pt, and Pd–Pt appear. These new metallic bonds conduct to a partial electronic transfer from Pd to Pt. Another phenomenon to take into account when discussing the increase in the concentration of $Pd^{\delta+}$ species after reduction of the catalysts is the migration of Pd to the outer surface of the alloyed particles. This can be indirectly evidenced by XPS when comparing the surface atomic concentration of $Pd^{\delta+}$

species and the bimetallic Pd–Pt catalysts in the calcined and reduced states (Table 4). Making the assumption that an increase in the atomic concentration of the different surface species is indicative of a higher exposition of the surface atoms to XPS, i.e. higher dispersion, the observed increase in $Pd^{\delta+}$ atomic surface concentrations for the bimetallic catalysts after reduction can be interpreted as the dispersion of the $Pd^{\delta+}$ species augmenting after reduction. As the $Pd^{\delta+}$ species are a part of the Pd–Pt alloyed particles a very plausible explanation of this behavior is the migration of Pd atoms to the outer surface of the particles.

Regarding the effect of residual chlorine in the oxidation state of the metals, both XPS (Table 4) and TPR (Fig. 4) showed its presence on both the calcined and reduced catalysts. One evidence of the effect of residual chlorine on the oxidation state of the metals is the fact that the Pt 4f line was found to be fully overlapped with the Al 2p line of the γ-Al_2O_3 support (not shown). The reason for this is the high resistance to reduction of the oxo-chlorided-platinum complexes formed during calcination [52]. Previous reports [56,57] have determined that such separation is only feasible when a significant amount of Pt particles is in the metallic Pt^0 oxidation state. Such condition is very difficult to achieve in catalysts with a Pt metallic content below 2 wt.% prepared from chlorided precursors [56]. On the other hand, the TPR (Fig. 4) for the Pd–Pt catalysts displayed peaks corresponding to the signals assigned to chlorine species (HCl and Cl^+). Such peaks can be ascribed to oxo-chlorided-Pt and -Pd complexes formed during the calcination stage [52,55,58–60]. These complexes are more refractory to reduction compared to the Pt and Pd oxides. TPR showed that Pd is more easily reduced than Pt. The evolvement profile of chlorine species from Pd(1.9) was even less complex than the one registered for Pt(1.3). The intense MS Cl^+ peak of Pd was located at the same position (467 K) of the H_2 reduction curve which was at a lower temperature than the peak for Pt. As observed in Fig. 4c–f the production of chlorine species was lower for the bimetallic Pd–Pt/γ-Al_2O_3 catalysts than for Pt and Pd. The signals of chlorine species for Pd–Pt catalysts had their maxima around 500–505 K for all the alloys excepting Pd(1.0)–Pt(0.5) for which such maximum was at a lower temperature (442 K). Moreover, compared to the other alloys this catalyst exhibited the strongest peak for the Cl^+ and HCl signals. The works presented in the literature demonstrate that after reduction the residual chlorine is not directly attached to the metals [58], but its presence facilitates the formation of stronger Pt,Pd–O–Al bridges between the metal and the support [59]. In such bonds the more intimate contact between the metal and the support can lead to an ionization of the metals resulting in electron-deficient metallic particles [58–61]. Finally, XPS results showed that the surface Cl/Al atomic ratio increases after reduction. Considering the arguments presented above such increase can be interpreted as an increase in the dispersion of residual chlorine on the reduced catalysts. It can be speculated that such increase is a result of the elimination of chlorine during the reduction process and simultaneously to a migration of chlorine atoms from the proximities of the metallic phases to other sites of the alumina carrier.

The above-presented evidence leads to conclude that important changes are occurring on the surface of the Pd–Pt alloyed particles from the calcined to the reduced state. From the results of characterization presented so far, the surface of the reduced Pd–Pt catalysts; which constitutes the activation step of the catalysts before the HDS reaction tests, is pictured as a complex mixture of electron-deficient $Pd^{\delta+}$ species located in the outer shell of the alloyed particles, interacting with a metallic core constituted by Pd and Pt atoms and strongly bound to the alumina carrier. Over the surface of the latter residual chlorine is also present. This picture is in the same line of the propositions presented by other authors [19,20,62–64]. In particular, Fujikawa et al. [64] proposed that the active phase of Pd–Pt in aromatics hydrogenation under H_2S atmospheres consists on "Pd dispersed on Pt particles". The contribution of the present work in this sense is that it was possible to establish the chemical nature of the Pd species mentioned in the literature.

Considering the evidence presented so far and the aspects discussed about the mechanism of the HYD route, we propose that over the Pd–Pt alloys the hydrogenation–dehydrogenation steps involved in HYD are mainly taking place over the electron-deficient $Pd^{\delta+}$ atoms located at the shell of the alloyed Pd–Pt particles and the withdrawal of the S heteroatom, as referred either to the C–S–C bond scission step in HYD or to the DDS route, from the adsorbed reaction intermediates mainly occurs on core Pt atoms. This does not rule out neither the existence of intermetallic Pd–Pt active sites acting as hydrogenation and S withdrawal active sites nor the existence of Pd particles performing S withdrawal from DBT (DDS) and its partially hydrogenated intermediates (HYD). Adsorption of H_2S and sulfur over such $Pd^{\delta+}$ sites does not occur due to their high electron deficiency which significantly reduces noble metal affinity with the electron-acceptor S atom. This proposition can well explain the synergy in HYD observed and the strong dependence of the catalytic performance of the Pd–Pt bimetallic systems in HDS on the Pd/(Pd + Pt) molar ratio. The model of a Pd–Pt active phase conformed and operating in the way proposed above reconciles the results obtained here for the HDS of dibenzothiophene and those reported for the hydrogenation of aromatics under H_2S atmospheres (HDA) and is supported by experimental data presented in the literature. Several authors have proposed that the main hydrogenation active sites of the bimetallic Pd–Pt alloys are Pd atoms keeping their metallic character under HDT reaction conditions [14,19,65]. Under sulfidation conditions it has been found that a mixture of metallic, Pt, Pd, and Pd–Pt particles, and sulfided PtS_x and PdS_x species exists [19,55,66,67]. According to the results of Qian et al. [67] the sulfur accommodated on the noble metals is highly labile and participates in the HDS reaction. Bando et al. [66] demonstrated that sulfidation of the Pd–Pt particles proceeds from the core of the alloy and that Pt atoms are more accessible to sulfur. Niquille-Röthlisberger and Prins [14] suggested that the highly active hydrogenating active sites responsible for the development of the HYD route of hydrodesulfurization were Pd atoms keeping their metallic character. Finally, it must be remarked that the sulfided Pd and Pt species are neither thermodynamically stable [19,29] nor is the strength of the Pt–S and Pd–S bonds high enough to form an active phase consisting of sulfur uncoordinated vacancies as those corresponding to MoS_2-based systems [67]. Nevertheless, in an analogous way, some recent studies [8,68] indicate that the active site for HYD on MoS_2-based catalysts possesses a metallic character (so-called "Brim-sites") [8] and do not adsorb H_2S [8,67].

A last consideration related to the nature of the synergy effect observed for the Pd–Pt/γ-Al_2O_3 catalysts in both the HYD route and HDA has to do with the effect of residual chlorine, which in addition to its influence in the oxidation state of the metals can, according to the literature, enhance the acidic properties of γ-Al_2O_3 promoting the creation of additional metal–support interface sites active for hydrogenation reactions, and over which the aromatics can be adsorbed [69,70].

3.3. Influence of naphthalene and H_2S on the HDS of dibenzothiophene over Pd–Pt/γ-Al_2O_3

Fig. 5 shows the results of the long-run test performed over a selected Pd–Pt/γ-Al_2O_3 catalyst (Pd(1.0)–Pt(0.5)) as a function of time on stream. The addition of NP to the liquid feed during the HDS test significantly changed neither the activity (Fig. 5a) nor the selectivity in the hydrodesulfurization reaction (Fig. 5b). The

catalyst displayed a very high activity in the hydrogenation of NP, $\%C_{NP}$ c.a. 100%, and simultaneously kept its good selectivity to HYD. NP was converted mostly into TTL with low amounts of *cis*-DCL and *trans*-DCL (not shown). It must be noticed that the conversion of NP was always higher than that of DBT. Such differences have been ascribed to differences in resonance energies [71,72]. Comparing the present results with those previously reported [15,29], it is particularly remarked that Pt/γ-Al_2O_3 [29] is more selective to the hydrodesulfurization reaction than to NP hydrogenation, while an inverse trend is observed for Pd/γ-Al_2O_3 [15]. Further increase in the H_2S concentration caused an inhibition effect on both reactions, but did not change the Pd–Pt catalytic functionalities (Fig. 5). Accordingly, the selectivity remained invariable regarding either NP hydrogenation to DBT hydrodesulfurization or HYD to DDS, as in the case of monometallic Pt/γ-Al_2O_3 [29]. A slight increase in the production of both DBT partially hydrogenated intermediates was observed, in particular of the THDBT intermediate. This points out the fact that at very high H_2S concentrations the dynamics of the mechanism of DBT hydrodesulfurization over Pd–Pt can be modified. A similar behavior has been recently reported for unpromoted MoS_2 [11]. It is often considered that H_2S partial pressure has a more negative effect on DDS than on HYD [2,3,13,16,73,74]. The trend observed in Fig. 5b shows that over Pd–Pt alloyed catalysts, both reaction pathways are negatively affected by H_2S to a similar extent, and that by increasing H_2S partial pressure only partial hydrogenation of dibenzothiophene to THDBT is favored. Thus, it can be considered that HYD was stopped at this step. The shift in the dynamics of the simultaneous hydrogenation and desulfurization reactions caused by H_2S can be related to a modification in the rate of activation and transfer of hydrogen from the catalytic surface to the reacting molecules due to a partial blocking of the Pd–Pt active sites by sulfur [29,73,74]. Finally, after withdrawing the excess H_2S concentration from the reaction environment it was observed that the Pd–Pt catalyst recovers almost all of its initial activity only merely changing its selectivity. It is interesting to observe in Fig. 5b that while the yield of HHDBT and THDBT remained at the same level than in the stage under high H_2S concentration, the gap between the yields of CHB and BP widened, as compared to the initial stages of the reaction test, in favor of the latter. This indicates that a small but irreversible change in the dynamics of the HYD pathway has been caused by the introduction of DMDS and further increase in the H_2S partial pressure in the reaction environment. One probable cause for this is an increase in the amount of irreversible sulfur species over the catalyst due to the decomposition of DMDS into H_2S and CH_4. This is a likeable possibility since, in one hand we have estimated that at the conditions of the long-run experiment the partial pressure of H_2S produced by the hydrodesulfurization of DBT (average steady state conversion ≈ 65%) is c.a. 10 kPa. After the introduction of DMDS to the reactor H_2S partial augments until 20 kPa. The deposition of irreversible held sulfur under such conditions is known to occur. But, on the other hand the experiments conducted by Qian et al. [67] indicated that the amount of sulfur accommodated on alumina-supported Pd–Pt catalysts depends on the partial pressure of H_2S produced from the HDS of dibenzothiophene and reaches equilibrium for when the amount of hydrodesulfurized DBT leads to levels of H_2S partial pressures higher than 7 kPa and up to 17 kPa. Therefore, not only the increase in the H_2S partial pressure but the nature of the organosulfur molecule can play a role in the phenomenon. Indeed, previous literature works have presented evidence indicating that DMDS is a more effective sulfiding agent than DBT [75]. Consequently, during the period of time of the experiment when DMDS is present it was possible that its decomposition can lead to a further increase in the amount of irreversible held sulfur. Regardless of the precise cause of the registered trend, the results in this work point out that H_2S mostly has a strong inhibitory effect rather than severe poisoning on the catalytic performance of the Pd–Pt alloyed particles in HDT, as some other authors have documented [19,67].

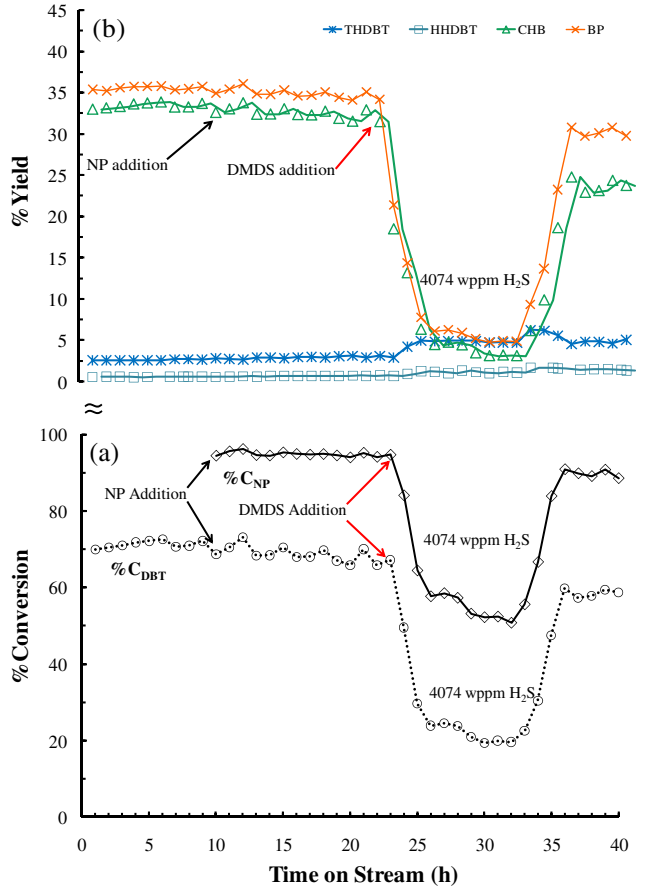

Fig. 5. Effect of the addition of NP and subsequent increase of H_2S concentration in the evolution of the performance of Pd(1.0)–Pt(0.5) catalyst (Pd/(Pd + Pt) molar ratio = 0.8) with time on stream during a desulfurization long-run test: (a) conversion of DBT and NP, and (b) products distribution. Additional H_2S concentration in the reaction atmosphere c.a. 4074 wppm.

4. Conclusions

The hydrodesulfurization of DBT over Pd–Pt/γ-Al_2O_3 catalysts as a function of the Pd/(Pd + Pt) molar ratio was studied at different reaction conditions. It was determined that no strong synergy effects on the HDS activity over the Pd–Pt alloyed system exist. Instead, a synergetic effect for the development of the HYD route of desulfurization was observed in agreement with the synergy of Pd–Pt in aromatics hydrogenation under an H_2S atmosphere. The mechanism of HYD was proposed to be a dynamic competition between hydrogenation–dehydrogenation C–S–C bond breaking reactions related somehow to the rate of hydrogen activation and transfer from the catalytic surface to the adsorbed reactant molecules which can be controlled from the Pd/(Pd + Pt) molar ratio of the alloy due to geometric effects. Characterization results showed that the development of HYD is related to the existence of a Pd–Pt active phase where electron-deficient $Pd^{\delta+}$ atoms are responsible for the hydrogenation–dehydrogenation steps involved in HYD and the withdrawal of the S heteroatom mainly takes place on Pt sites.

On the other hand, the addition of NP during HDS was found to change neither the HDS activity nor the HYD selectivity.

When increasing H_2S concentration in the reaction environment an inhibition of all catalytic functionalities of Pd–Pt was observed rather than poisoning. This inhibition effect hinders the C–S–C bond scission step of both the HYD and DDS reaction pathways.

Acknowledgments

This work was possible due to the financial support of COLCIENCIAS, a government institution that promotes science and technology in Colombia, in the frame of the Project 1102-06-17636. V.G. Baldovino-Medrano thanks COLCIENCIAS for a Ph.D. scholarship.

References

[1] C. Song, Catal. Today 86 (2003) 211.
[2] D.D. Whitehurst, T. Isoda, I. Mochida, Adv. Catal. 42 (1998) 345.
[3] M.V. Landau, D. Berger, M. Herskowitz, J. Catal. 159 (1996) 236.
[4] H. Yang, C. Fairbridge, Z. Ring, Energy Fuels 17 (2003) 387.
[5] H. Kwart, G.C.A. Schuit, B.C. Gates, J. Catal. 61 (1980) 128.
[6] M. Zdražil, Appl. Catal. 4 (1982) 107.
[7] P. Raybaud, J. Hafner, G. Kresse, H. Toulhoat, Phys. Rev. Lett. 80 (1998) 1481.
[8] F. Besenbacher, M. Brorson, B.S. Clausen, S. Helveg, B. Hinnemann, J. Kibsgaard, J.V. Lauritsen, P.G. Moses, J.K. Nørskov, H. Topsøe, Catal. Today 130 (2008) 86.
[9] R. Prins, M. Egorova, A. Röthlisberger, Y. Zhao, N. Sivasankar, P. Kukula, Catal. Today 111 (2006) 84.
[10] H. Wang, R. Prins, Appl. Catal. A: Gen. 350 (2008) 191.
[11] H. Wang, R. Prins, J. Catal. 258 (2008) 153.
[12] S. Cristol, J.-F. Paul, E. Payen, D. Bougeard, F. Hutschka, S. Clémendot, J. Catal. 224 (2004) 138.
[13] J. Mijoin, G. Pérot, F. Bataille, J.L. Lemberton, M. Breysse, S. Kasztelan, Catal. Lett. 71 (2001) 139.
[14] A. Niquille-Röthlisberger, R. Prins, J. Catal. 242 (2006) 207.
[15] V.G. Baldovino-Medrano, S.A. Giraldo, A. Centeno, J. Mol. Catal. A: Chem. 301 (2009) 127.
[16] F. Bataille, J.-L. Lemberton, P. Michaud, G. Pérot, M. Vrinat, M. Lemaire, E. Schulz, M. Breysse, S. Kasztelan, J. Catal. 191 (2000) 409.
[17] V.G. Baldovino-Medrano, S.A. Giraldo, A. Centeno, Información Tecnológica 20 (2009) in press.
[18] H.R. Reinhoudt, R. Troost, A.D. van Langeveld, S.T. Sie, J.A.R. van Veen, J.A. Moulijn, Fuel Proc. Tech. 61 (1999) 133.
[19] Y. Yoshimura, M. Toba, T. Matsui, M. Harada, Y. Ichihashi, K.K. Bando, H. Yasuda, H. Ishihara, Y. Morita, T. Kameoka, Appl. Catal. A: Gen. 322 (2007) 152.
[20] N. Matsubayashi, H. Yasuda, M. Imamura, Y. Yoshimura, Catal. Today 45 (1998) 375.
[21] W. Palczewska, Adv. Catal. 24 (1975) 245.
[22] S. Hermans, C. Diverchy, O. Demoulin, V. Dubois, E.M. Gaigneaux, M. Devillers, J. Catal. 243 (2006) 239.
[23] R.M. Navarro, B. Pawelec, J.M. Trejo, R. Mariscal, J.L.G. Fierro, J. Catal. 189 (2000) 184.
[24] L.M. Tosta Simplício, S. Teixeira Brandão, E. Andrade Sales, L. Lietti, F. Bozon-Verduraz, Appl. Catal. B: Environ. 63 (2006) 9.
[25] H. Karhu, A. Kalantar, I.J. Väyrynen, T. Salmi, D.Yu. Murzin, Appl. Catal. A: Gen. 247 (2003) 283.
[26] J. Haber, Pure Appl. Chem. 63 (1991) 1227.
[27] M.L. Vrinat, Appl. Catal. 6 (1983) 137.
[28] E. Dhainaut, H. Charcosset, C. Cachet, L. de Mourgues, Appl. Catal. 2 (1982) 75.
[29] V.G. Baldovino-Medrano, S.A. Giraldo, A. Centeno, Fuel 87 (2008) 1917.
[30] M. Egorova, R. Prins, J. Catal. 225 (2004) 417.
[31] G.H. Singhal, R.L. Espino, J.E. Sobel, J. Catal. 67 (1981) 446.
[32] M. Houalla, N.K. Nag, A.V. Sapre, D.H. Broderick, B.C. Gates, AlChE J. 24 (1978) 1015.
[33] C.-M. Wang, T.-C. Tsai, I. Wang, J. Catal. 262 (2009) 206.
[34] A.W. Weitkamp, Adv. Catal. 18 (1968) 1.
[35] S. Dokjampa, T. Rirksomboon, S. Osuwan, S. Jongpatiwut, D.E. Resasco, Catal. Today 123 (2007) 218.
[36] A.K. Neyestanaki, P. Mäki-Arvela, H. Backman, H. Karhu, T. Salmi, J. Väyrynen, D.Yu. Murzin, J. Mol. Catal. A: Chem. 193 (2003) 237.
[37] M. Breysse, E. Furimsky, S. Kasztelan, M. Lacroix, G. Pérot, Catal. Rev. Sci. Eng. 44 (2002) 651.
[38] S. Khoobiar, J. Phys. Chem. 68 (1964) 411.
[39] Y. Wang, R.T. Yang, J. Catal. 260 (2008) 198.
[40] A.K. Neyestanaki, P. Mäki-Arvela, H. Backman, H. Karhu, T. Salmi, J. Väyrynen, D.Yu. Murzin, J. Catal. 218 (2003) 267.
[41] Balint, A. Miyazaki, K.-i. Aika, Chem. Mater. 13 (2001) 932.
[42] T.-B. Lin, C.-A. Jan, J.-R. Chang, Ind. Eng. Chem. Res. 34 (1995) 4284.
[43] E. Guillon, J. Lynch, D. Uzio, B. Didillon, Catal. Today 65 (2001) 201.
[44] E.O. Orozco, M. Vrinat, Appl. Catal. A: Gen. 170 (1998) 195.
[45] H. Conrad, G. Ertl, J. Koch, E.E. Latta, Surf. Sci. 43 (1974) 462.
[46] M. Boudart, Adv. Catal. 20 (1969) 153.
[47] C.M. Friend, D.A. Chen, Polyhedron 16 (1997) 3165.
[48] L. Guczi, Z. Schay, Stud. Surf. Sci. Catal. 27 (1986) 313.
[49] M. Jacquin, D.J. Jones, J. Rozière, A.J. López, E. Rodríguez-Castellón, J.M.T. Menayo, M. Lenarda, L. Storaro, A. Vaccari, S. Albertazzi, J. Catal. 228 (2004) 447.
[50] H. Jiang, H. Yang, R. Hawkins, Z. Ring, Catal. Today 125 (2007) 282.
[51] L. Fiermans, R. De Gryse, G. De Doncker, P.A. Jacobs, J.A. Martens, J. Catal. 193 (2000) 108.
[52] H. Lieske, G. Lietz, H. Spindler, J. Völter, J. Catal. 81 (1983) 8.
[53] N.K. Nag, J. Phys. Chem. B 105 (2001) 5945.
[54] I.T. Caga, J.M. Winterbottom, J. Catal. 57 (1979) 494.
[55] K.K. Bando, T. Matsui, Y. Ichihashi, K. Sato, T. Tanaka, M. Imamura, N. Matsubayashi, Y. Yoshimura, Phys. Scr. T115 (2005) 828.
[56] J.Z. Shyu, K. Otto, Appl. Surf. Sci. 32 (1988) 246.
[57] Z. Paál, P. Tétényi, M. Muhler, U. Wild, J.-M. Manoli, C. Potvin, J. Chem. Soc. Faraday Trans. 94 (1998) 459.
[58] S.D. Jackson, J. Willis, G.D. Mclellan, G. Webb, M.B.T. Keegan, R.B. Moyes, S. Simpson, P.B. Wells, R. Whyman, J. Catal. 139 (1993) 191.
[59] A. Sarkany, G. Stefler, J.W. Hightower, Appl. Catal. A: Gen. 127 (1995) 77.
[60] A. Stanislaus, B.H. Cooper, Catal. Rev. Sci. Eng. 36 (1994) 75.
[61] W.M.H. Sachtler, A.Y. Stakheev, Catal. Today 12 (1992) 283.
[62] K. Persson, A. Ersson, K. Jansson, J.L.G. Fierro, S.G. Järås, J. Catal. 243 (2006) 14.
[63] L. Hilaire, G. Diaz Guerrero, P. Légaré, G. Maire, G. Krill, Surf. Sci. 146 (1984) 569.
[64] T. Fujikawa, K. Tsuji, H. Mizuguchi, H. Godo, K. Idei, K. Usui, Catal. Lett. 63 (1999) 27.
[65] B. Coq, F. Figueras, J. Mol. Catal. A: Chem. 173 (2001) 117.
[66] K.K. Bando, T. Kawai, K. Asakura, T. Matsui, L. Le Bihan, H. Yasuda, Y. Yoshimura, S.T. Oyama, Catal. Today 111 (2006) 199.
[67] E.W. Qian, K. Otani, L. Li, A. Ishihara, T. Kabe, J. Catal. 221 (2004) 294.
[68] V. Vanrysselberghe, G.F. Froment, Ind. Eng. Chem. Res. 35 (1996) 3311.
[69] P. Chou, M.A. Vannice, J. Catal. 107 (1987) 129.
[70] A.Yu. Stakheev, L.M. Kustov, Appl. Catal. A: Gen. 188 (1999) 3.
[71] B. Pawelec, R. Mariscal, R.M. Navarro, S. van Bokhorst, S. Rojas, J.L.G. Fierro, Appl. Catal. A: Gen. 225 (2002) 223.
[72] S. Jongpatiwut, Z. Li, D.E. Resasco, W.E. Alvarez, E.L. Sughrue, G.W. Dodwell, Appl. Catal. A: Gen. 262 (2004) 241.
[73] H. Farag, Appl. Catal. A: Gen. 331 (2007) 51.
[74] V. Rabarihoela-Rakotovao, S. Brunet, G. Perot, F. Diehl, Appl. Catal. A: Gen. 306 (2006) 34.
[75] S. Texier S, G. Berhault, G. Pérot, V. Harlé, F. Diehl, J. Catal. 223 (2004) 404.